EasyChair Preprint

№ 10286

Design and Control of a Tele-Operated Soft Instrument in Minimally Invasive Surgery

Jialei Shi and Helge Wurdemann

May 29, 2023

Design and Control of a Tele-operated Soft Instrument in Minimally Invasive Surgery

J. Shi[1] and H. Wurdemann[1]

[1]*Mechanical Engineering, University College London, UK*
h.wurdemann@ucl.ac.uk

INTRODUCTION

The medical sector has emphasised increasing levels of autonomy to achieve safe and efficient robot-assisted surgeries [1]. In this case, robust and intuitive manipulation of medical robots is crucial, and many tele-operated surgical robots have been developed, e.g., the da Vinci robotic platform. The tele-operation can offer high operation precision and intuitive manipulation. In addition, soft robots have led to the development of inherently safe and flexible interventional tools for medical applications, e.g, the minimally invasive surgery (MIS). Soft instruments are particular advantageous to navigate in tortuous anatomical environments with constrained space [2]. Combining the tele-operation technology with soft robots might further result in a significant reduction in operation time and increase of surgeons' dexterity [3]. The contribution of this work lies in the design and control of a tele-operated soft instrument for laparoscopic examination are proposed based on the miniaturised STIFF-FLOP manipulators (with a diameter of 11.5 mm) [4]. Specifically, the robot has two serially connected modules, which can seamlessly fit to commercially available 12 mm trocar ports used in MIS (see Fig. 1). The bending angle of the soft instrument can achieve 180°. We also preliminarily validate the feasibility of the soft instrument.

MATERIALS AND METHODS

A. System Overview

The robot body is made of a low shore hardness silicone (Ecofex 00-50 Supersoft, SmoothOn). The robot has six fully fiber-reinforced circular chambers distributed evenly. Two adjacent chambers are internally connected via a 1 mm silicone pipes and actuated as one pair. An inner lumen of a 4.5 mm diameter is preserved to feed through a 4 mm endoscope camera (OV9734, China). The length of one robot module is 55 mm (see Fig. 1). The soft instrument is tele-operated by the Touch X (Geomagic, US). The command pose y_d is calculated by the relative linear position displacement of the Touch X,

$$y_d = k_d(y_c - y_s), \tag{1}$$

where y_s is the start position when the tele-operation begins, y_c is the current position and k_d is a 3×3 diagonal gain matrix to adjust the scale of the robot motion.

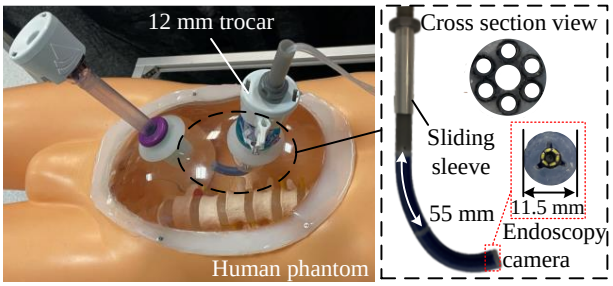

Fig. 1 (a) Human phantom with 12 mm disposable trocar ports. (b) The soft instrument has two identical robot segments, a 4 mm endoscopy camera is integrated at the tip of the robot. A sliding sleeve is designed to fully open the sealing part of the trocar before inserting the robot.

A PC with the Robot Operating System (ROS) is used as the host to achieve communication between the Touch X and a laptop running Matlab for achieving inverse kinematics, the calculated desired pressure is sent to an Arduino Due to regulate the chamber pressure via pressure regulators (Camozzi K8P, Italy).

B. Inverse Kinematic Control

The spatial configuration of the robot's backbone can be described using a displacement vector $p(s)$ and a rotation matrix $R(s)$. Differentiating them with respect to the curve length s, denoted by $(\cdot)_{,s}$. This yields

$$p_{,s}(s) = R(s)v(s), \quad R_{,s}(s) = R(s)\hat{u}(s), \tag{2}$$

where $v(s)$ and $u(s)$ are the local strain vector and curvatures, with $\hat{u}(s)$ as a skew-symmetric matrix. The derivatives of force $n(s)$ and moment $m(s)$ are

$$n_{,s}(s) = f_e(s)+f_P(s),\ m_{,s}(s) = -\hat{p}_{,s}n(s)-l_e(s)+l_P(s), \tag{3}$$

where $f_e(s)$ and $l_e(s)$ are the distributed external force and moment. $f_P(s)$ and $l_P(s)$ are the distributed force and moment resulting from pressurisation and equal

$$f_P(s) = \sum_{i=1}^{6}[P^i A_c R_s(s)e_3], \quad m_P(s) = \sum_{i=1}^{6} P^i A_c R(s)[(v(s) + \hat{u}(s)d^i) \times e_3 + \hat{d}^i\hat{u}(s)e_3)], \tag{4}$$

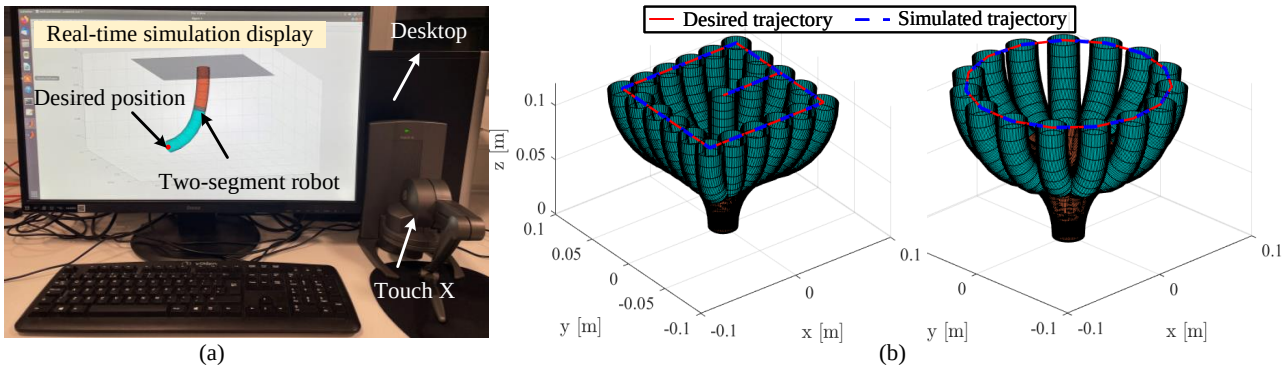

(a) (b)

Fig. 2 (a) The simulated robot is visualised via Matlab interface and controlled by the Touch X. (b) The simulation results for the inverse kinematics when tracking a rectangular (side width of 120 mm) and circular shape (diameter of 160 mm), and the tip of the robot is kept vertically for demonstration.

where P^i is the pressure in the ith chamber, A_c is the chamber area, $\hat{d}^i$ is the position vector of the ith chamber, $e_3 = [0, 0, 1]$. A linear constitutive material model is adopted to relate $n(s), m(s)$ to $v(s), u(s)$, yielding in (5)

$$n(s) = R(s)K_{se}(v(s) - e_3^T), \quad m(s) = R(s)K_{bt}u(s), \quad (5)$$

where K_{se} contains the shear and elongation stiffness, and K_{bt} contains the bending and torsion stiffness.

1) Boundary Conditions: For a two-segment robot with the length of L_1 and L_2, the boundary conditions of the force and moment at the tip of the robot are

$$n(t^-) = F_P(t^-) + F_e(t^+), \; m(t^-) = m_P(t^-) + m_e(t^+), \quad (6)$$

where $t = L_1 + L_2$, the subscripts P and e denote the force and torque from the pressurisation and external. Considering a rigid connection between two segments, the intermediate boundary conditions need to be satisfied

$$\begin{aligned} n(L_1^-) &= F_P(L_1^-) + n(L_1^+) + F_e(L_1^-) - F_P(L_1^+), \\ m(L_1^-) &= m_P(L_1^-) + m(L_1^+) + m_e(L_1^-) - m_P(L_1^+), \end{aligned} \quad (7)$$

where the superscripts $^-$ and $^+$ denote the left and right limits. For the inverse kinematics, the desired configuration can be y_d and R_d. As such,

$$p(t) = y_d, R(t) = R_d. \quad (8)$$

2) Numerical Implementation: The shooting method can then be applied by assuming the initial guess as

$$g(0) = [n(0), m(0), P], \; s.t. \; P_{max} > P^i > 0, \; i = 1 \cdots 6. \quad (9)$$

where $n(0)$ and $m(0)$ are the force and moment at the base, P contains the actuation pressure in six chambers and P_{max} is the maximum allowed pressure. Specifically, by integrating (2) and (3) (using the fourth-order Runge–Kutta method) based on the initial condition (9) and satisfying (7)-(8). The problem is solved as a nonlinear least-square problem via Matlab.

RESULTS

The feasibility of the soft instrument is validated via a human phantom equipped with 12 mm trocar ports (see Fig. 1). The sliding sleeve can successfully prevent the robot directly interacting with the sealing part of the trocar during the insertion process. As such, the robot doesn't suffer from buckling. In addition, the sliding sleeve is retractable to guarantee the sealing quality once the robot has passed. The simulation is visualised by Matlab, where the desired tip position is controlled by the Touch X (see Fig. 2(a)). The demonstration of the inverse kinematic control is exemplified by using two trajectories, i.e., rectangular and circular shapes. The tip of robot is kept towards the z-axis. The results are shown in Fig. 2(b), which shows the fidelity of the invsere control.

DISCUSSION

Compared with the robots from e.g., [2], [4] (diameter of 14.5 mm), our soft instrument (diameter of 11.5 mm) has the smallest diameter. This miniaturised dimension enables the robot seamlessly fit to the commonly available 12 mm trocar. The proposed inverse kinematic control is applicable to control the tip position and orientation with a frequency between 15-20 Hz in our PC (Intel i5, RAM 32 GB). It is worth mentioning that the problem generally can be solved within 3-5 optimisation iterations. As such, it is possible to improve the computation performance, e.g., using C++. We have also created soft robots with diameter of 8 mm. As such, we will further scale down the system dimension. In addition, we will evaluate the intuitiveness of the tele-operation system based on user tests and experimentally validate the accuracy of the inverse kinematic control.

REFERENCES

[1] G.-Z. Yang, J. Cambias, K. Cleary, E. Daimler, and et al., "Medical robotics—regulatory, ethical, and legal considerations for increasing levels of autonomy," p. eaam8638, 2017.

[2] A. Diodato, M. Brancadoro, G. De Rossi, and et al., "Soft robotic manipulator for improving dexterity in minimally invasive surgery," vol. 25, no. 1, pp. 69–76, 2018.

[3] A. Arezzo, Y. Mintz, M. E. Allaix, and et al., "Total mesorectal excision using a soft and flexible robotic arm: a feasibility study in cadaver models," *Surgical endoscopy*, vol. 31, pp. 264–273, 2017.

[4] J. Shi, W. Gaozhang, and H. A. Wurdemann, "Design and characterisation of cross-sectional geometries for soft robotic manipulators with fibre-reinforced chambers," in *Proc. IEEE Int. Conf. Soft Robot.*, 2022, pp. 125–131.